Solidification Crack Susceptibility in Weld Metals of Fully Austenitic Stainless Steels (Report III)†

—Effect of Strain Rate on Cracking Threshold in Weld Metal during Solidification—

Yoshiaki ARATA*, Fukuhisa MATSUDA*, Hiroji NAKAGAWA, Seiji KATAYAMA*** and Seishiro OGATA******

Abstract

The present study was undertaken to obtain a better understanding of solidification and ductility-dip crackings[1),2),3)] occurring in fully austenitic stainless steel weld metals of SUS 310S using a combination of the Slow-Bending speed type Trans-Varestraint test and a fractographic method by the scanning electron microscopy. The cracking threshold curve showing the nucleation property of solidification cracking was first obtained by varying combinations of strains and stain rates, so that the cracking threshold curve appeared to be almost identical with the ductility curve of BTR showing the propagation property of solidification cracking obtained by the Trans-Varestraint test. The solidification crack was likely to occur because of the lowest ductility in spite of the strain rate within the higher temperature range of the BTR over which the crack surface morphology showed a dendritic appearance as an evidence of liquid, while ductility-dip cracking became unlikely to occur as the strain rate decreased. Moreover, it is concluded that the surface morphology of solidification cracks was divided into three distinct types and was closely related to the separation temperature at which cracking occurred in spite of the effects of the augmented-strain and the strain rate.

1. Introduction

In the previous report[1)] the hot crack susceptibility of austenitic stainless steel weld metals was evaluated by determining the ductility curves during welding by the Trans-Varestraint test. As a result fully austenitic AISI310S (Japanese Industrial Standard (JIS); SUS-310S) exhibited the wide BTR (solidification brittleness temperature range) during weld solidification from about 1400 to about 1250°C, the low ε_{min} (the minimum augmented-strain required to cause solidification cracking) and in addition the wide DTR (ductility-dip temperature range) from about 1200 to 850°C, while austenitic AISI304 (JIS; SUS304) containing residual δ-ferrite exhibited the narrow BTR and the high ε_{min} and did not exhibit the DTR. Therefore, it was recognized that SUS310S weld mteals were very susceptible to solidification cracks and might also possess a possibility to form ductility-dip cracks although SUS304 weld metals were resistant to hot cracks such as solidification and ductility-dip cracks. However, by the Trans-Varestraint test which applies an appropriate augmented-strain to a weld metal very quickly and causes hot cracks to occur in the weld metal almost simultaneously, it is impossible to know the properties of the occurrence and propagation of cracks when the strain rate, in fact, changes variously.

On the other hand, the hot cracking test called the Slow-Bending Speed type Trans-Varestraint test (the SB Trans-Varestraint test) by which a given augmented-strain can be applied to the weld metal at various strain rates was newly developed and was utilized for Aluminum alloy weld metals[4)].

According to the report[4)], in some alloys such as 5083, 5052, etc. the minimum augmented-strain value required to cause a cracking threshold was raised in case of lower strain rate in comparison with the conventional Trans-Varestraint test. Practically, it is rather the rare case that the stresses or strains exerted in the weld metals during welding change as suddenly as those of the Trans-Varestraint test. From the above reasons, in the present study the newly developed SB Trans-Varestraint test was used for the fully austenitic SUS310S susceptible to solidification and ductility-dip crackings in order to investigate the effect of strain rates on the mechanism and the formation tendency of these crackings. Furthermore, a fractographic investigation was carried out using a scanning electron microscope (SEM) to see distinctly the presence of

† Received on November 1, 1977

* Professor
** Research Instructor
*** Graduate student, Osaka University
**** Former graduate student, now with Sumitomo Heavy Industries LTD.

Table 1 Chemical composition of commercially available plates of SUS 310S investigated

Material (SUS)	Composition (wt%)								
	C	Si	Mn	P	S	Cr	Ni	Mo	Cu
310S	0.08	0.94	1.58	0.022	0.007	24.66	20.37	0.10	0.04

solidification and ductility-dip cracks, the difference between them, and the features of the surface morphology of crackings.

2. Experimental Procedure

2.1 *Material used*

The material used for this investigation was commercially available SUS310S of $100\times100\times3$ mm plates, the composition of which is shown in **Table 1.** SUS310S weld metal is well known to show the fully austenitic microstructure and to be susceptible to hot cracking.

2.2 *Slow-Bending Speed type Trans-Varestraint test (SB Trans-Varestraint test)*

The SB Trans-Varestraint apparatus[4], an improvement on the conventional Trans-Varestraint apparatus, can exert various strain rates on the surface of a specimen by controlling the falling speed of the yokes. The augmented-strains and the strain rates were applied on the specimen surface by the falling distance of yokes and by dropping the yokes at an appropriate speed respectively. The strains measured beforehand by a strain gauge and an electromagnetic oscillograph were varied from about 0.02 to 3%, and the strain rates were from about 0.2 to 60%/sec.

The SB Trans-Varestraint test was performed during welding under the same conditions. Then the welding conditions were 100 amp, 12–13 volt, 150 mm/min of dcsp TIG arc bead-on-plate welding.

2.3 *Fractography of hot cracks*

All the SB Trans-Varestraint specimens were examined using the scanning electron microscope (SEM) to understand the morphology of cracks and the presence of a ductility-dip crack. The specimens less than 20 mm in length were cut from the SB Trans-Vrestraint specimens to contain hot cracks. These were first observed from the surface and then were fractured by bending repeatedly at room temperature to investigate the fracture surface morphology in detail.

3. Result and Discussion

3.1 *Hot crackings in the SB Trans-Varestraint specimens*

The SB Trans-Varestraint test is characteristic of applying various strain rate ($\dot{\varepsilon}$) and enables us to investigate the effect of the strain rate on the susceptibility to hot crackings. An example of strain rates as a function of temperature after applying each strain used for this test is shown as the curves from the liquidus temperature against the ductility curve of SUS 310S weld metal obtained by the Trans-Varestraint test in **Fig. 1.** These curves were obtained by

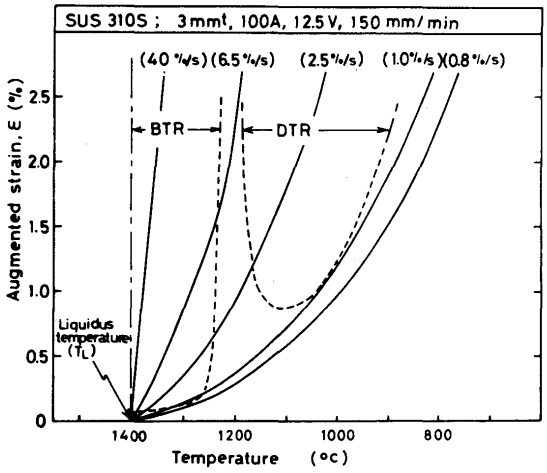

Fig. 1 Strain rates applied during SB Trans-Varestraint testing and ductility curve obtained by Trans-Varestraint test

coupling the strain rates as a function of time with the temperature distribution measured with a calibrated W·5%Re-W·26%Re thermocouples (0.3 mmϕ)[4]. The length and the fracture surface morphology of solidification cracks and the presence of ductility-dip cracks were investigated by varying augmented-strains at such strain rates as shown in Fig. 1. The examples of hot crackings formed at the strain (ε)=3.0% by the SB Trans-Varestraint test are shown in a low magnification in **Fig. 2**(a) ($\dot{\varepsilon}$=1.3%/sec), 2(b) ($\dot{\varepsilon}$=1.8%/sec), 2(c) ($\dot{\varepsilon}$=12.5%/sec) and 2(d) ($\dot{\varepsilon}$=60%/sec) and in addition the scanning electron microscope (SEM) photographs near the end of large solidification cracks are shown in low and high magnifications in **Fig. 3**(a),

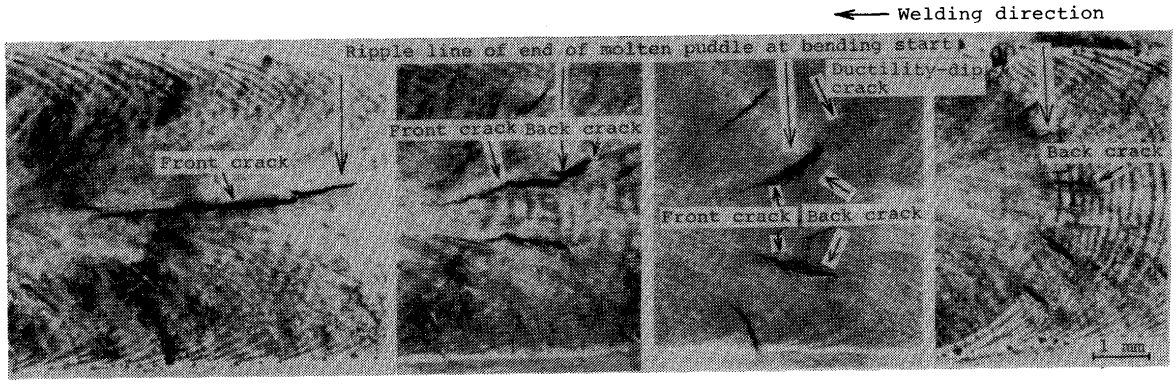

Fig. 2 Macrographs of solidification and ductility-dip cracks occurring at strain of 3% in SB Trans-Varestraint specimens of SUS 310S weld metals as a function of strain rate (a); 1.3%/sec, (b); 1.8%/sec, (c); 12.5%/sec and (d); 60%/sec

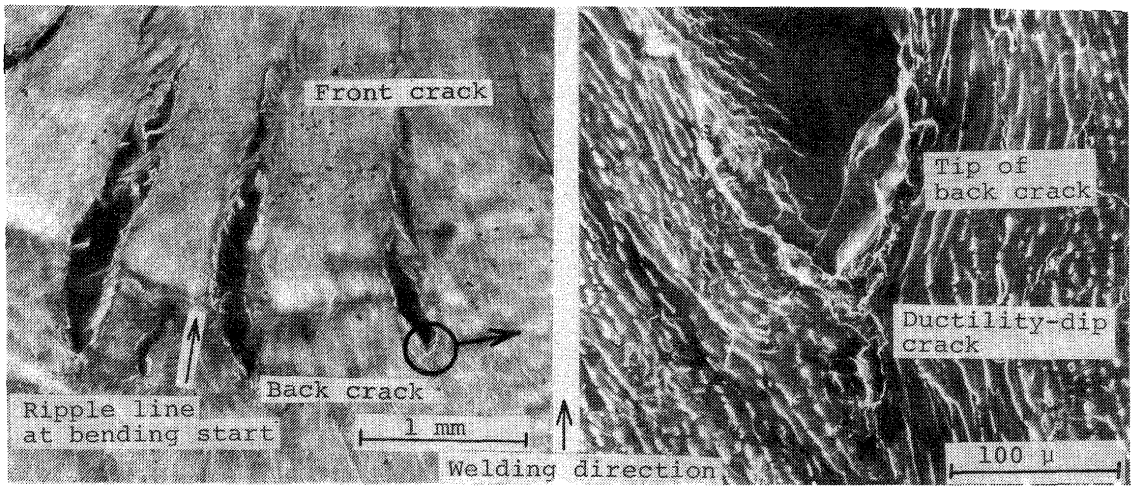

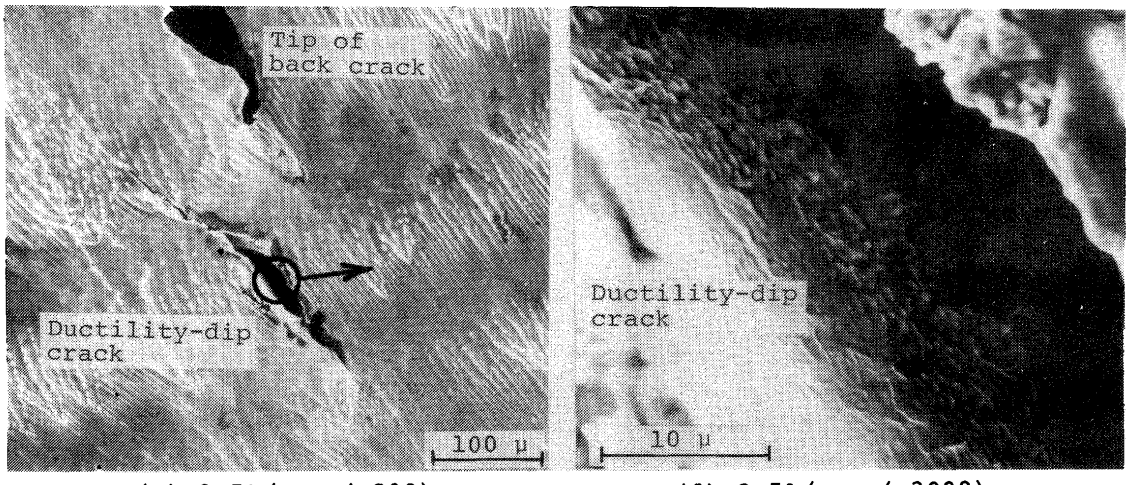

Fig. 3 SEM micrographs of solidification and ductility-dip cracks at $\varepsilon=3.0\%$—ductility-dip crack at tip of solidification crack at $\dot{\varepsilon}=6.5\%$/sec, (a); ×30, (b); ×300, and ductility-dip crack a little way off solidification crack at $\dot{\varepsilon}=2.5\%$/sec, (c); ×200, (d); ×3000

(b) ($\dot{\varepsilon}$=6.5%/sec), and (c), (d) ($\dot{\varepsilon}$=2.5%/sec).

Large solidification cracks in the SB Trans-Varestraint specimens were mainly formed almost perpendicular to and across the ripple line at the time when the strain started to be applied. Judged by the ripple line, the cracks toward the welding direction are called "Front Crack" and the ones toward the reverse are "Back Crack". The maximum length of a solidification crack adding the front crack and the back crack without a ductility-dip crack along the welding direction is called "Whole Crack length". The whole crack length at ε=3.0% is plotted to study the effect of the strain rate on the length in **Fig. 4.** The solid line

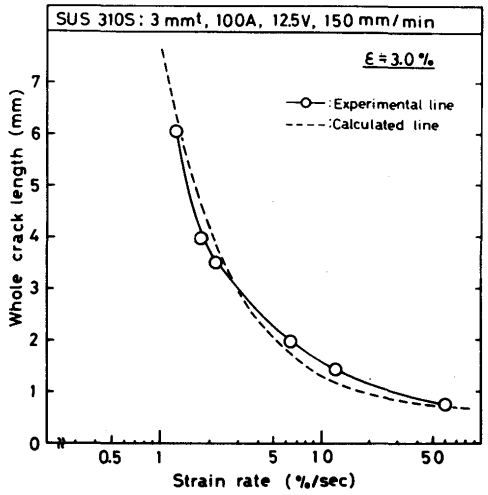

Fig. 4 Effect of strain rate on solidification crack length in SB Trans-Varstraint specimens and solid line showing experimental result in comparison with broken line showing length of solidification crack introduced from expression considering ductility curve of BTR

drawn from the results shows that the whole crack length increased as the strain rate decreased. The back crack is generally thought to have occurred within the BTR lower than the crossing temperature at which the strain rate intersected the ductility curve of the BTR, while the large front crack is thought to have formed due to the molten puddle moving toward the welding direction accompanied by the BTR while the strain was being applied more and more to a given level at a constant strain rate after the occurrence of a crack threshold and the subsequent back crack. The maximum strain rate of the SB Trans-Varestraint test corresponds to that of the conventional Trans-Varestraint test. The front cracks in the Trans-Varestraint specimens were very short or might not occur, as shown in Fig. 2(c). This is probably why the strain was exerted to the given level so quickly that the BTR hardly moved toward the welding direction during the application of the strain. On the basis of the above consideration the expression of the whole crack length (L_W) at each strain rate can be introduced from the ductility curve of the Trans-Varestraint test as follows[5]:

$$L_W = L_B + L_F = l_B + V(\varepsilon_u - 2\times\varepsilon_{min})/\dot{\varepsilon} \quad (1)$$

Here, L_W ; length of Whole Crack (mm)
L_B ; length of Back Crack (mm)
L_F ; length of Front Crack (mm)
l_B ; length of crack corresponding to BTR occurring at a simultaneous strain rate (mm)
V ; welding speed (mm/sec)
ε_{min} ; minimum augmented-strain required to cause cracking (%)
ε_u ; given augmented-strain (%)
$\dot{\varepsilon}$; given strain rate (%/sec)

Supposing that ε_u=3.0 (%), ε_{min}=0.08(%), V=2.5 (mm/sec) and l_B=0.6 (mm) in the expression (1), the whole crack length was calculated by varying the strain rates. The result is drawn as the broken line, so that it shows the tendency in good agreement with the experimental result. Therefore, the introduced expression (1) is available as well as the ductility curve obtained by the Trans-Varestraint test is of significance. Such an appearance of solidification cracks show the same tendency as the aluminum alloys already reported[4,5]. However, in addition to these solidification cracks in SUS310S weld metals, small ductility-dip cracks were found at the end of and a little way off the back cracks toward the reverse of the welding direction as shown in Fig. 2(c) and Fig. 3(a) to (d). Fig. 3(b) of the higher magnification of Fig. 3(a) and Fig. 3(d) of the higher magnification of Fig. 3(c) show the examples of the formation of ductility-dip cracks at the end of the back crack and a little way off the back crack respectively. The fracture surface of ductility-dip cracks was characteristic of the intergranular cracking mode and the smoothness in low magnifications coated with much smaller solids than protuberances of dendritic arms showing the rough appearance in high magnification as shown in Fig. 3(d). The fracture surface morphology of solidification cracks will be described for further details in 3.3 and 3.4.

3.2 *Effect of strain rate on threshold of hot cracking*

It was carried out to investigate the presence of solidification and ductility-dip crackings at different augmented-strains and strain rates. The results are

plotted in **Fig. 5**, in which the mark in crack-free case is shown as ○, the mark of the occurrence of either solidification crack or ductility-dip crack is ● or □ respectively, and in the case of the both occurrence it is ◙. The regions of the strain and the strain rate within which solidification and ductility-dip crackings occurred were determined as Region I and Region II respectively through the points representing the existence of cracks. Moreover, utilizing the results of Fig. 5, the solidification cracking threshold curve was

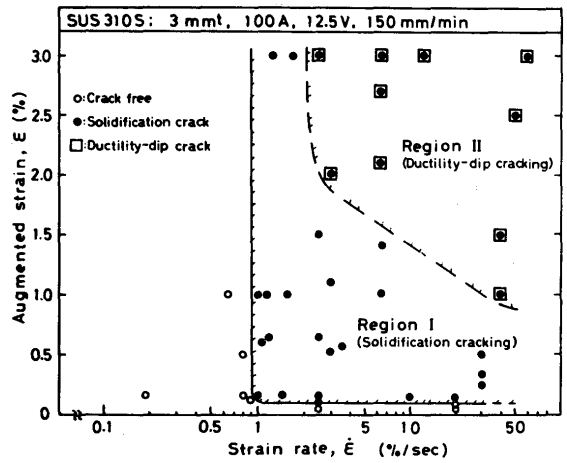

Fig. 5 Effects of augmented-strain and strain rate on nucleation or initiation of solidification and ductility-dip cracks

obtained in **Fig. 6**, in addition to the broken line of the ductility curve determined by the conventional Trans-Varestraint test. The strain rates are represented as the curves from the liquidus (T_L) against the temperature drop, on which the marks showing the presence of cracks are plotted again.

According to these results, the solidification cracking threshold curve almost corresponds to the ductility curve obtained by the Trans-Varestraint test. It is, therefore, recognized that solidification cracks tended to occur at a very low augmented-strain of 0.08% which hardly varied although the strain rates changed from about 20 to 1%/sec, and that the cracks could not be formed even at high augmented-strains at slower strain rates than the critical strain rate, 0.9%/sec, corresponding to the CST[6] in the Trans-Varestraint test because the slower strain rates did not intersect the ductility curve of solidification cracking threshold as shown in Fig. 6.

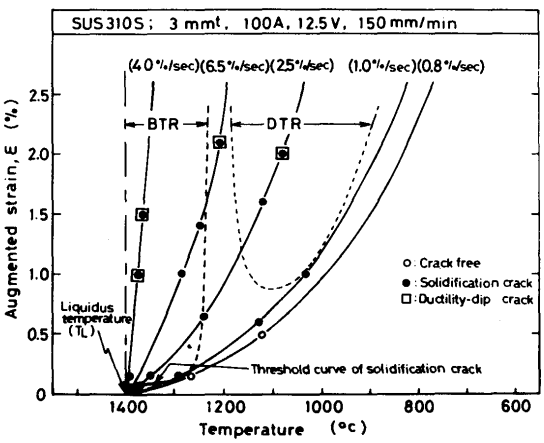

Fig. 6 Cracking threshold curve of SUS 310S weld metal obtained by SB Trans-Varestraint test

On the other hand, there was a tendency for ductility-dip cracks to become difficult to occur because the ε_{min} required to cause ductility-dip cracking increased considerably according to the decrease in the strain rate. Moreover, Region II is included by Region I as shown in Fig. 5. It is taken for granted from the above-mentioned results that it is solidification cracking that predominantly constitutes the greater practical problem, while ductility-dip cracking is scarcely considered to occur in the practical production.

3.3 *Effect of strain rate on fracture surface morphology at solidification cracking threshold*

The fracture surfaces of solidification cracks are discussed below using the SEM because solidification cracking appears to play a dominant role in the practical crack formation.

Fig. 7 shows a solidification crack surface formed almost simultaneously at a very rapid strain rate by Trans-Varestraint test[7),8)]. The welding direction is to the left. The features of the crack surface morphology are changing gradually from a dendritic to a smooth appearance according to the temperature drop from the left of the highest temperature separation to the right of the lower temperature separation.

On the basis of such distinct features that are closely related to the separation temperatures on account of the ratio of the liquid existing in interdendritic boundaries to the solid solidifying from the liquid, the fracture surface morphology is divided into three main regions[8),9)] as follows:—

1. Type D where the primary and the secondary arms of the cellular dendrites can be discerned and protuberances of dendritic arms are extending like tears upward from the surface near the liquidus temperature.
2. Type D-F where the protuberances of the secondary arms are turning into an obscure appearance although the primary dendrites are still distinguished.
3. Type F where a smooth or flat appearance with a

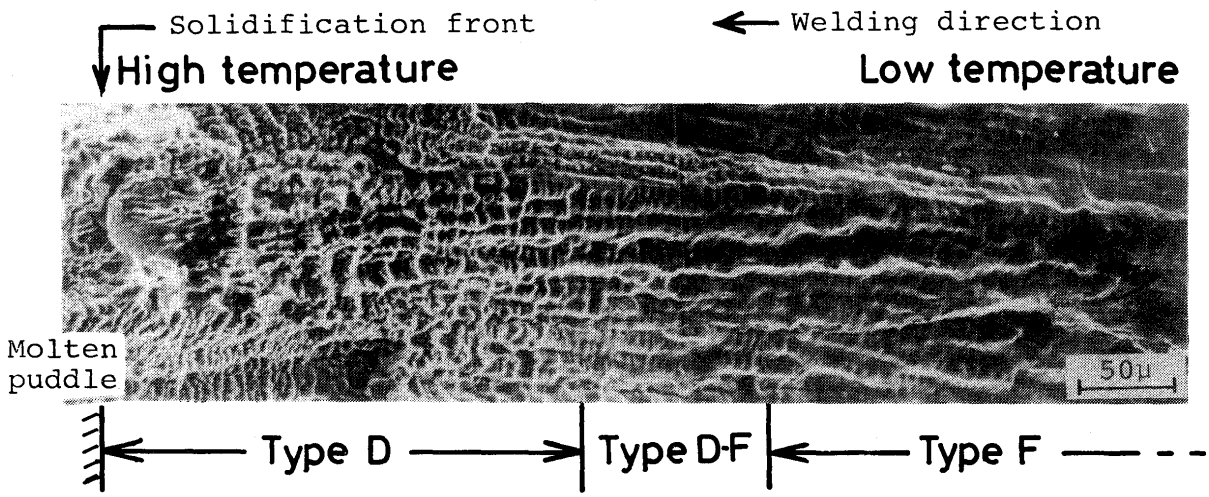

Fig. 7 SEM micrograph of solidification crack surface in Trans-Varestraint specimen of SUS 310S showing features from a dendritic mode to a smooth appearance depending on temperatures

number of small holes relative to the liquid is observed almost all over the surface.

The classification of the crack morphology such as Type D, Type D-F, and Type F is shown in conjunction with the cracking threshold curve and the ductility curve in **Fig. 8.** It appears possible to infer the

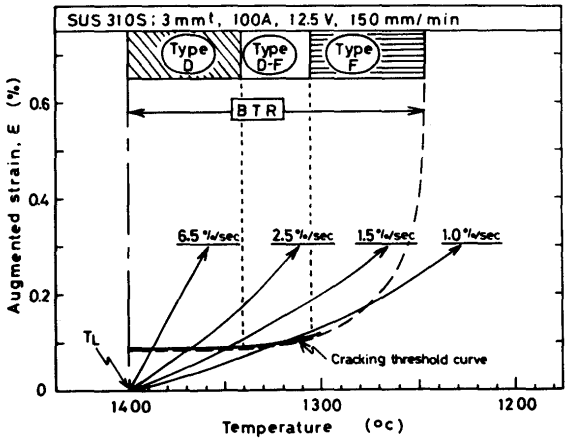

Fig. 8 Intersection between strain rate and ductility curve of cracking threshold suggesting effect of strain rate on separation temperature of cracking and crack surface morphology

cracking threshold temperature and the fracture surface morphology roughly from Fig. 8. For example, in the case of the strain rate of 2.5%/sec, the crossing temperature of the strain rate curve and the ductility curve is about 1370°C and consequently the fracture surface morphology at the cracking threshold is inferred to be Type D. In this way, in the case that the strain rate is 6.5, 1.5 or 1.0%/sec, the morphology ought to be Type D of a higher temperature, Type D of the lowest temperature, or typical Type D-F respectively corresponding to each intersecting temperature.

Since a cracking threshold could be judged by the noticeable ripple line corresponding to the end of the molten puddle at the moment when the strain started to be applied, the fracture surface morphology at the cracking threshold was investigated and is shown at each strain rate in **Fig. 9.** It is clear that Fig. 9 is in good accordance with the above inference from Fig. 8 as expected. It is, therefore, suggested from the results of Figs. 8 and 9 that a solidification crack in commercial SUS 310S weld metals should nucleate within the temperature range from about 1400 to about 1300°C and is difficult to occur due to an increase in ductility below about 1300°C as far as the cracking threshold is formed. Consequently it is natural to note that the morphology of solidification crack surface is chiefly Type D or Type D-F depending on the strain rate at the cracking threshold.

3.4 *Effect of strain rate on propagation properties of solidification crack*

3.4.1 *Propagation property of Back Crack*

In the SB Trans-Varestraint test the front cracks and the back cracks occurred as described in 3.1. It is reasonable to suppose that the both cracks occurred in the process of propagation after the cracking threshold initiated. Therefore, the propagation property of the back crack was first investigated because the crack was thought to have occurred by the same mechanism that solidification cracks in the Trans-

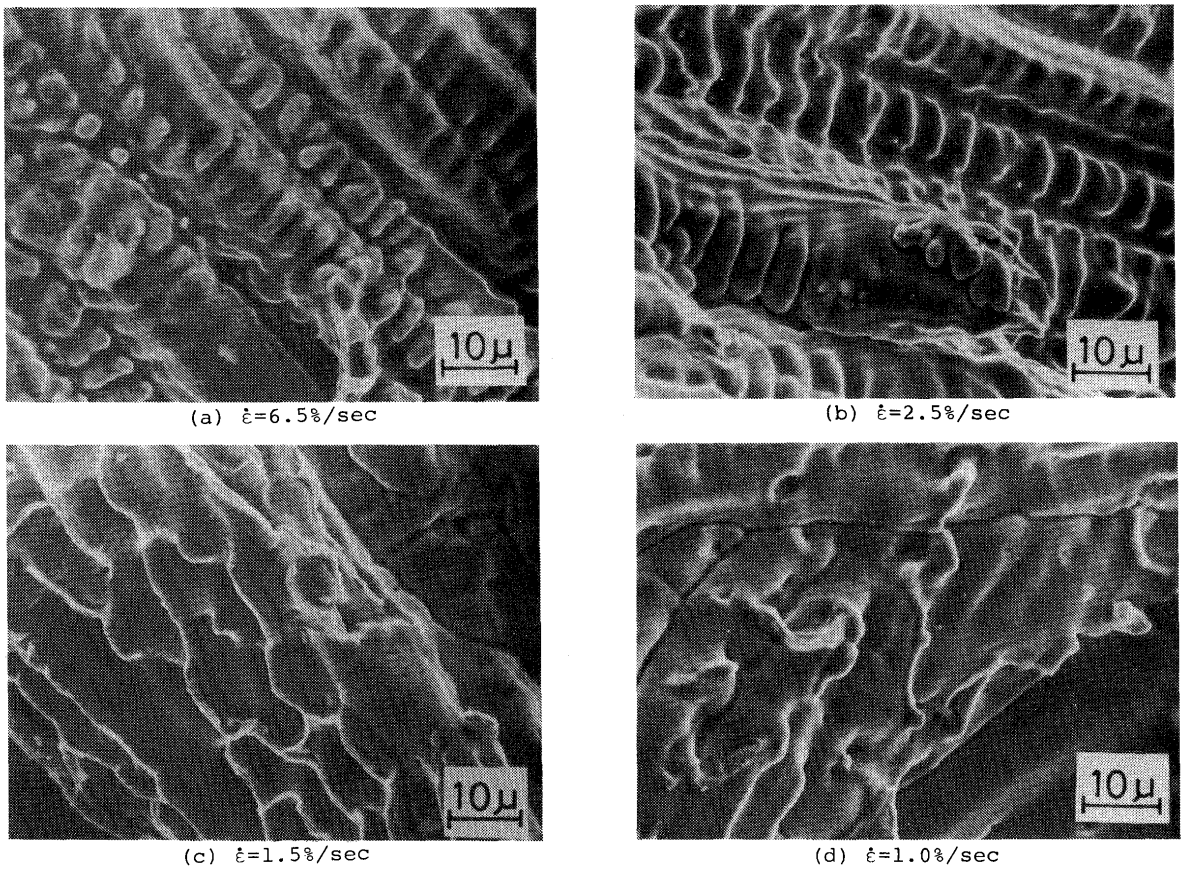

Fig. 9 SEM micrographs showing effect of strain rate on fracture surface morphology at cracking threshold—(a); $\dot{\varepsilon}=6.5\%$/sec, (b); $\dot{\varepsilon}=2.5\%$/sec, (c); $\dot{\varepsilon}=1.5\%$/sec and (d); $\dot{\varepsilon}=1.0\%$/sec

Varestraint test had nucleated at higher temperature near the liquidus and had propagated to the lower temperature regions within the BTR.[10] The examples of the crack surfaces are shown in the case of the strain rates of 1.0 and 2.5%/sec at the augmented-strain of 0.6% in **Fig. 10.**

The crack surface morphology was observed to be Type D-F and Type F at $\dot{\varepsilon}=1.0\%$/sec and Type D, Type D-F and Type F at $\dot{\varepsilon}=2.5\%$/sec from the features changing from higher to lower temperatures.

These results are in good agreement with the inferable results probably because the back crack occurred within the BTR below the crossing temperature which was estimated at about 1320°C at $\dot{\varepsilon}=1.0\%$/sec and at about 1370°C at $\dot{\varepsilon}=2.5\%$/sec from Fig. 8 in 3.3, except that the back crack length became shorter than expected as the strain rate decreased. It was clear as a result of observing the crack surfaces that the region of Type F characterized by a smooth surface was narrowed in the case of slow strain rates, so that the arrested temperature of crack propagation backward was, strictly speaking, shifted and raised from the lowest temperature (about 1240°C) of the BTR to about 1280°C according to the decrease in the strain rate. Moreover, in the condition that the augmented-strain was applied slightly higher above the ε_{min}, the back crack was arrested at a still higher temperature in spite of the strain rate. It is suggested from these results that the Type F region has the greater resistance to the propagation of a solidification crack. Furthermore, it implies the other point of view that the observation that the area of Type F is narrow in practical cracking formation corresponds to the case of a very low strain and/or a very slow strain rate.

3.4.2 *Propagation property of Front Crack*

The examples of the crack surface at $\varepsilon=0.15\%$ a little above ε_{min} are shown in **Fig. 11.** The greatest part of the crack surface belonged to the back crack and the front crack was very small because of the very low strain. This result appears to mean that a solidification crack may not propagate forward so rapidly and long when the strain is no longer applied, although it can propagate backward at a very rapid speed immediately after the nucleation.

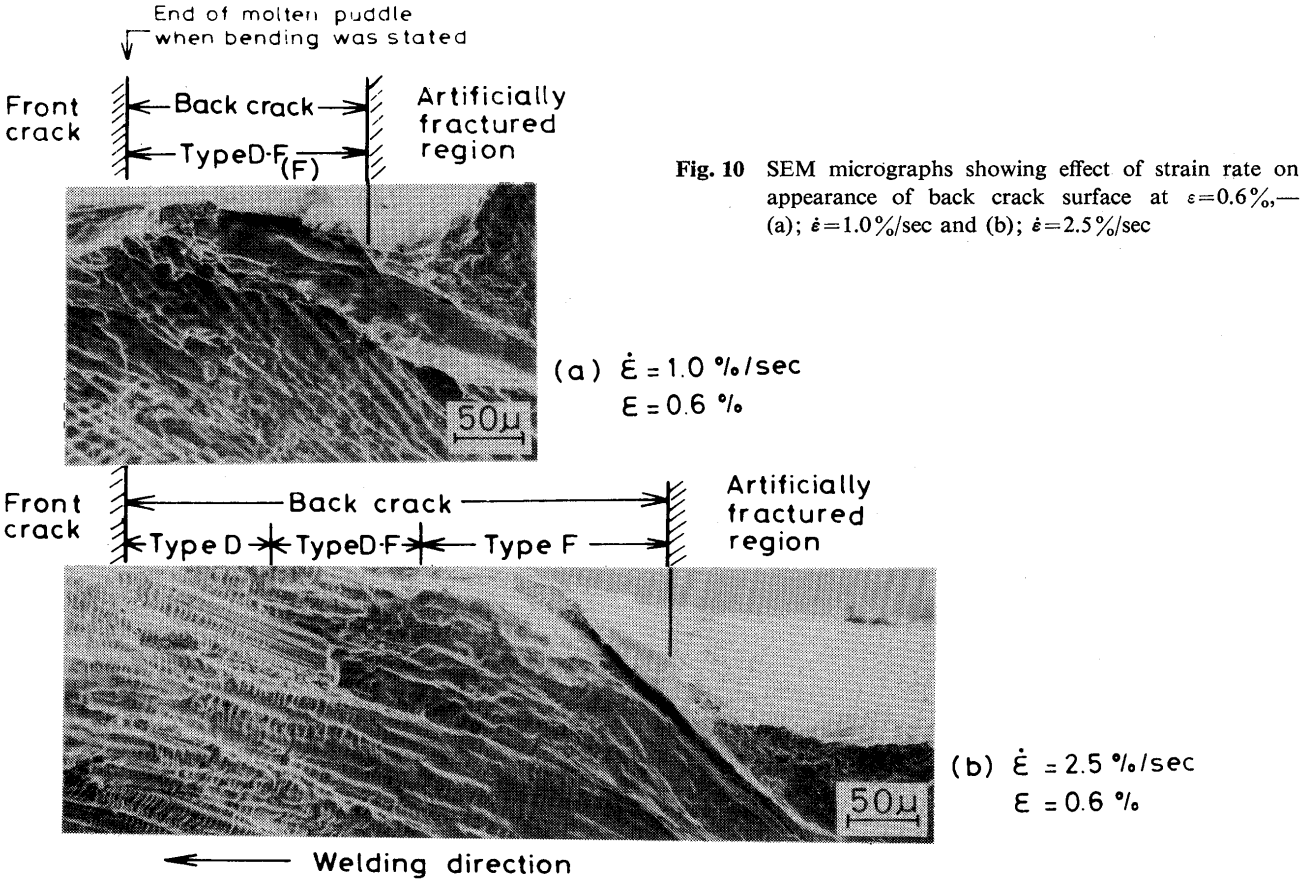

Fig. 10 SEM micrographs showing effect of strain rate on appearance of back crack surface at ε=0.6%,— (a); $\dot{\varepsilon}$=1.0%/sec and (b); $\dot{\varepsilon}$=2.5%/sec

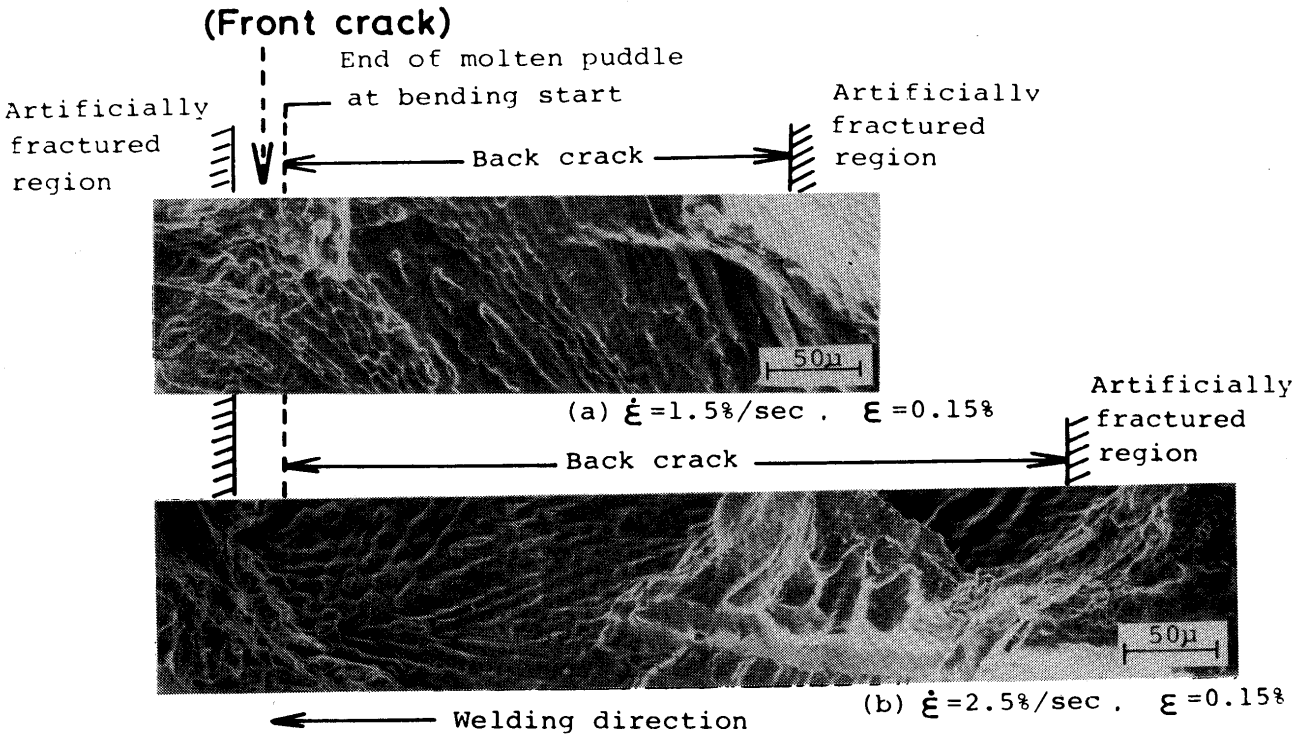

Fig. 11 SEM micrographs showing appearance of front crack in case of ε=0.15% slightly higher than ε_{min} in conjunction with large back crack,— (a); $\dot{\varepsilon}$=1.5%/sec and (b); $\dot{\varepsilon}$=2.5%/sec

Fig. 12 shows the typical surface morphology of the front crack under the different conditions of strains and strain rates in a high magnification. It is easily observed that the morphology was Type D at $\dot{\varepsilon}$=6.5 and 2.5%/sec and Type D-F at $\dot{\varepsilon}$=1.0%/sec and did not depend on the strains. That is to say, the morphology of the front crack was hardly affected by the strain but by the strain rate; the morphology was changing from Type D to Type D-F as the strain rate decreased. The morphology during propagating forward was the same as the morphology at the cracking threshold, so that this phenomenan appears similar to the mechanism described using Fig. 8 in 3.3. It indicates after all that the morphology of the front crack depends generally on the crossing temperature relative to the ductility curve of materials and the strain rate when the strain required to cause cracking is over the critical strain of ε_{min}. Moreover, it is judged from the results of Figs. 8, 11 and 12 that the tip of the front crack proceeding toward the welding

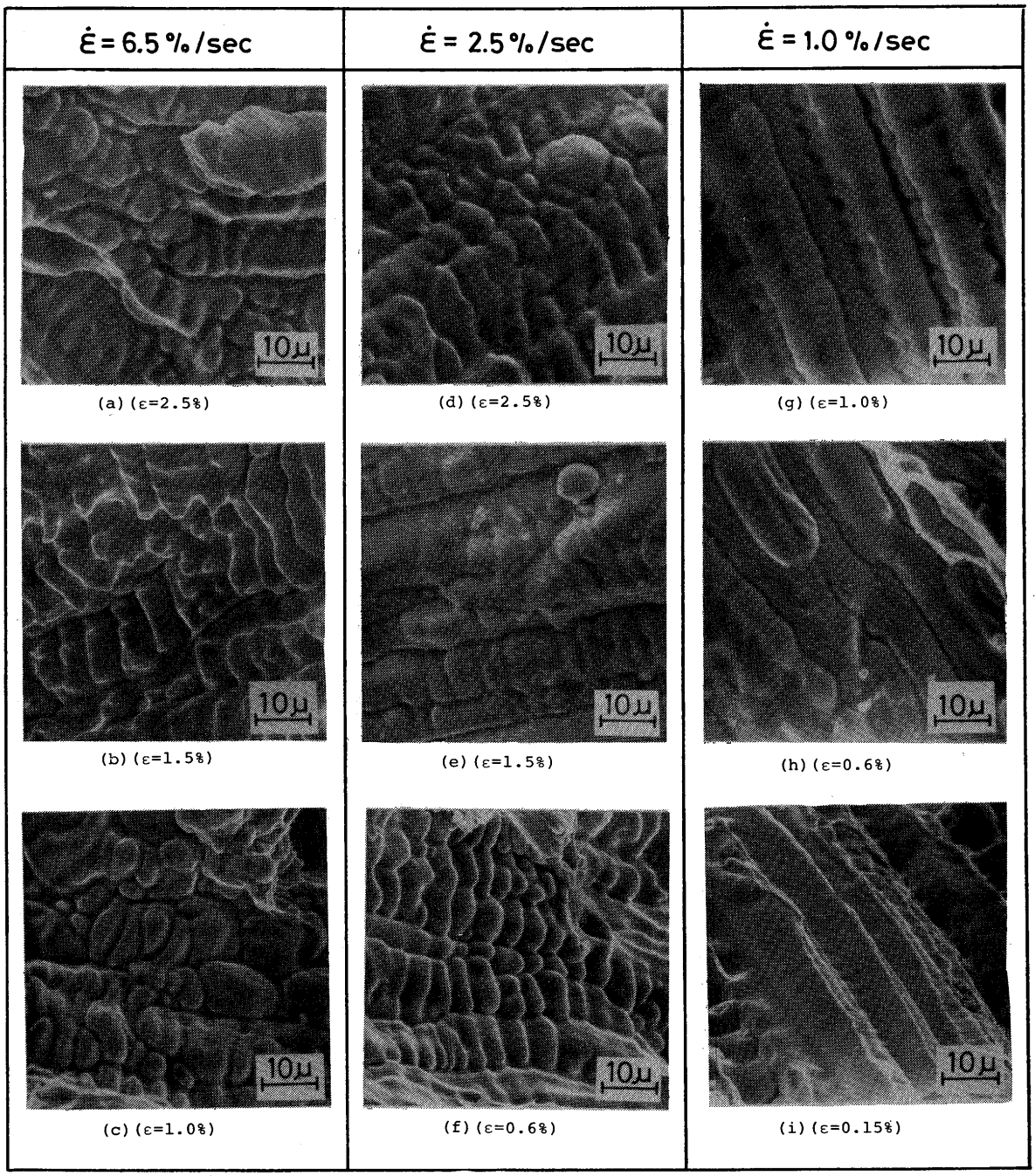

Fig. 12 SEM micrographs showing effects of strain and strain rate on surface morphology of front crack

direction was propagating at about the same constant speed as the welding speed near the crossing temperature at which the crack had nucleated.

As a result of the observation of crack surfaces in 3.3 and 3.4, the factor determining the crack surface morphology depends not on the strain and the strain rate but predominantly on the separating temperature of cracking inferred by the strain rate. This will be indeed useful in observing hot crackings in other tests and in practical services to infer roughly the circumstances of crackings.

4. Conclusions

The Slow-Bending speed type Trans-Varestraint test and the fractographic examination were performed to investigate the effect of the strain rate on solidification and ductility-dip crackings in commercial SUS 310S weld metals.

The conclusions drawn are as follows;

(1) Solidification cracking occurred above the very low augmented-strain of about 0.1% in spite of the variation of the strain rate from 20 to about 0.9%/sec, but on the other hand ductility-dip cracking became unlikely to nucleate as the strain rate decreased because the minimum augmented-strain required to cause cracking was greatly raised accordingly. It is, therefore, suggested that it is the solidification cracking that constitutes the greatest practical problems on cracking in fully austenitic stainless steel weld metals.

(2) As a result that a solidification crack was divided into the Front Crack and the Back Crack by the cracking threshold, the formation of the solidification crack is generally understood from the model that the back crack first occurred almost simultaneously from the threshold to the lower temperature within the BTR and later the front crack was formed because the BTR of the very low ε_{min} following the molten puddle proceeded toward the welding direction while the more strain was being applied in the case of the faster strain rate than 0.9%/sec.

(3) As a result of the observation of the solidification crack surface, the crack surface morphology was divided into three distinct types according to the features changing from a dendritic mode to a smooth appearance. It is, moreover, concluded that the morphology was not affected by the strain and the strain rate but depended only on the separating temperature at which the crack occurred. The broad regions of the dendritic morphology showing the evidence of a considerable amount of liquid appeared to be responsible for the reduction in ductility because the areas of the smooth surface were influenced by the strain and the strain rate; the areas were narrowed accordingly as the strain and/or the strain rate decreased.

References

1) Y. Arata, F. Matsuda and S. Katayama: "Solidification Crack Susceptibility in Weld Metals of Fully Austenitic Stainless Steels (Report II)", Trans. JWRI, Vol. 6 (1977) No. 1, pp. 105–116.
2) B. Hemsworth, T. Boniszewski and N. F. Eaton: "Classification and Definition of High Temperature Welding Cracks in Alloys", Metal Const. & Brit. Weld. J., (1969) Feb., pp. 5–16.
3) J. Heneycombe and T. G. Gooch: "Microcracking in Fully Austenitic Stainless Steel Weld Metal", Metal Const. & Brit. Weld. J., (1970) Sept., pp. 375–379.
4) Y. Arata, F. Matsuda, K. Nakata and K. Shinozaki: "Solidification Crack Susceptibility of Aluminum Alloy Weld Metals (Report II)", Trans. JWRI, Vol. 6 (1977) No. 1, pp. 91–104.
5) Y. Arata, F. Matsuda, K. Nakata and K. Shinozaki: "Solidification Crack Susceptibility of Aluminum Alloy Weld Metals (Report III)", Trans. JWRI, Vol. 6 (1977) No. 2.
6) T. Senda, F. Matsuda, et al.: "Fundamental Investigations on Solidification Crack Susceptibility for Weld Metal with Trans-Varestraint Test", Trans. of JWS, Vol. 2 (1971) No. 2, pp. 1–22.
7) F. Matsuda and H. Nakagawa: "Some Fractographic Features of Various Weld Cracking and Fracture Surfaces with Scanning Electron Microscope (Report I)", Trans. JWRI, Vol. 6 (1977) No. 1, pp. 81–90.
8) Y. Arata, F. Matsuda, K. Nakata and I. Sasaki: "Solification Crack Susceptibility of Aluminum Alloy Weld Metals (Report I)", Trans. JWRI, Vol. 5 (1976) No. 2, pp. 53–67.
9) F. Matsuda et al.: "Some Fractographic Features of Various Weld Metal Cracking and Fracture Surfaces with Scanning Electron Microscope", to be published in Trans. JWRI.
10) T. Senda, F. Matsuda and G. Takano: "Studies on Solidification Crack Susceptibility for Weld Metals with Trans-Varestraint Test (2)", J. of JWS, Vol. 42 (1973) No. 1, pp. 48–56.